

## SPECTROSCOPIC REDSHIFTS FOR SEVEN LENS GALAXIES

ERAN O. OFEK,<sup>1</sup> DAN MAOZ,<sup>1</sup> HANS-WALTER RIX,<sup>2</sup> CHRISTOPHER S. KOCHANÉK,<sup>3</sup> AND EMILIO E. FALCO<sup>4</sup>*Draft of February 5, 2008*

## ABSTRACT

We report Very Large Telescope observations of 11 lensed quasars, designed to measure the redshifts of their lens galaxies. We successfully determined the redshifts for seven systems, five of which were previously unknown. The securely measured redshifts for the lensing galaxies are: HE0047–1756  $z = 0.408$ ; PMNJ0134–0931  $z = 0.766$ ; HE0230–2130  $z = 0.522$ ; HE0435–1223  $z = 0.455$ ; SDSS0924+021  $z = 0.393$ ; LBQS1009–025  $z = 0.871$ ; and WFIJ2033–472  $z = 0.658$ . For four additional systems (BRI0952–0115, Q1017–207, Q1355–2257 and PMNJ1632–003) we estimate tentative redshifts based on some features in their spectra.

*Subject headings:* cosmology: gravitational lensing — Quasars: general — Quasars: individual: HE0047–1756, PMNJ0134–0931, HE0230–2130, HE0435–1223, SDSS0924+021, BRI0952–0115, LBQS1009–025, Q1017–207, Q1355–2257, PMNJ1632–003, WFIJ2033–472

## 1. INTRODUCTION

The roughly 90 known gravitational lens systems are powerful tools for studying cosmology, galaxy structure and galaxy evolution. Most systems have been observed with the *Hubble Space Telescope* (HST) to obtain precise photometry and astrometry, and increasing numbers have time delay measurements, measurements of microlensing variability, and determinations of the velocity dispersion of the lens galaxy. However, about 60% of the systems still lack the most basic parameters needed to use a lens as an astrophysical tool – the lens and/or source redshifts.

One important application of the lenses is to study the evolution of galaxy mass-to-light ratios. Gravitational lenses, unlike other samples of galaxies, are selected based on their masses, rather than their colors or surface brightnesses. By combining the masses of the lenses, as determined by lensing, with the photometry of the lens galaxies as determined from HST images, it is possible to measure directly the mass-to-light ratio of the lens population as a function of redshift (e.g., Treu et al. 2002; Rusin et al. 2003; Treu & Koopmans 2004; Rusin & Kochanek 2005). Rusin & Kochanek (2005), found that mass-selected lens galaxies show the same evolution rate as has been found for early-type galaxies in clusters (e.g., van Dokkum et al 1998; Pahre et al. 2001), and agree with the field evolution rates found by van Dokkum et al. (2001), but not with the faster rates found by Treu et al. (2002). The sample studied by the latter authors may have selection effects biasing it towards higher surface brightness, younger, systems. Many of the lens mass-to-light ratios have, however, large errors due to the uncertainties in their redshifts, increasing the errors in the estimated average evolution rate.

A second important application of lenses is to determine the surface density of dark matter and stars near the lensed

images, by measuring time delays between lensed images, and by monitoring for microlensing. Time delays determine the combination of physical variables  $\Delta t \propto H_0(1 - \langle \kappa \rangle)$  (Kochanek 2002), where  $H_0$  is the Hubble parameter,  $\langle \kappa \rangle = \Sigma/\Sigma_c$  is the mean surface density in the annulus between the images used to determine the time delay, normalized to the critical surface density,

$$\Sigma_c = \frac{c^2}{4\pi G} \frac{D_s}{D_l D_{ls}}. \quad (1)$$

The critical surface density is a function of the angular diameter distances  $D_s$ ,  $D_l$ , and  $D_{ls}$ , between the observer and source, observer and lens, and lens and source, respectively. Assuming  $H_0$  is known, measurements of time delays and microlensing variability can be used to determine the surface mass density and the fraction of that density in stars in the interesting regime where a galaxy is changing from being primarily stars to being dark-matter dominated.

A third application of lensed quasar systems which requires the lens galaxy redshifts is the estimation of the mass and number evolution of massive galaxies. For an unevolving comoving density of massive galaxies, the number of lenses is proportional to the volume out to the source, which is determined by cosmology (e.g., Mitchell et al. 2004). Thus, no-evolution models with large dark-energy content, which have a large volume out to a given source redshift, predict a large incidence of quasar lensing and a distribution of lens galaxy redshifts shifted to relatively high redshift. The currently favored cosmology ( $\Omega_m \simeq 0.3$ ,  $\Omega_\Lambda \simeq 0.7$ ) may predict too many lenses, given a non-evolving lens population (e.g., Maoz 2005). We can therefore turn the problem around; for a fixed cosmology, the only significant variables are the mass and number-density of massive galaxies, and their evolution (e.g., Ofek, Rix, & Maoz 2003; Chae et al. 2003). By analyzing samples having complete source and lens redshifts, it is possible to constrain the evolution rate of a mass-selected sample, without the problem of surface brightness selection effects that plague other samples.

In summary, each new lens redshift facilitates a wide array of astrophysical experiments. In this paper, we present European Southern Observatory (ESO) Very Large Telescope (VLT) Focal Reducer/Low Dispersion Spectrograph -

<sup>1</sup> School of Physics and Astronomy and the Wise Observatory, Tel-Aviv University, Tel-Aviv 69978, Israel. Electronic address: (eran, dani)@wise.tau.ac.il

<sup>2</sup> Max-Planck-Institut für Astronomie, Königstuhl 17, D-69117 Heidelberg, Germany

<sup>3</sup> Department of Astronomy, The Ohio State University, 140 West 18th Avenue, Columbus, OH 43210

<sup>4</sup> Harvard-Smithsonian Center for Astrophysics, 60 Garden Street, Cambridge, MA 02138

2 (FORS2) observations of 11 lensed systems, most of which lack lens galaxy redshift information. In seven cases the spectra yield reliable redshifts for the lensing galaxies. In §2 we describe the observations, the reduction, and the isolation and characterization of the lens galaxy spectra in the presence of strong contamination by lensed quasar light. The spectra and the measured redshifts for each galaxy are presented and discussed in §3.

## 2. OBSERVATIONS AND REDUCTION

We obtained low resolution spectra for 11 gravitationally lensed systems using the FORS2 spectrograph mounted on the VLT-Unit Telescope 1 at Paranal. We used a  $0''.7$ -wide slit and the 200I grism blazed at  $7450 \text{ \AA}$ , giving a wavelength range of  $5500 \text{ \AA}$  to  $9000 \text{ \AA}$ , a dispersion of  $2.5 \text{ \AA}$  per binned pixel, and  $\sim 5 \text{ \AA}$  full width at half maximum (FWHM) resolution. The MIT  $2k \times 4k$  pixel CCD was used, with on-chip binning of  $2 \times 2$ , giving a scale of  $0''.252$  per binned pixel. The observations were conducted in Service Mode on various dates, with an image quality varying between  $0''.5$  and  $0''.9$  FWHM. Table 1 lists, for each object, the observation date, the number of exposures and integration time per night, the total number of exposures, the total integration time, the seeing range and median in which the images were obtained, and the slit position angle.

Figure 1 shows HST images of each system, with the slit orientation and actual slit width overlaid. Even with the good seeing conditions at the VLT site, the lensing galaxy light is blended with light from one or more of the quasar images. The slit orientation was chosen to include, in addition to the lens galaxy, the lensed quasar image producing the dominant contamination. With a proper characterization of the contaminating image, we could then subtract it from the lens spectrum.

Image reduction was performed on the bias-subtracted and wavelength-calibrated images provided by ESO using MATLAB scripts specifically written by us for this purpose. The process included the following steps. First, cosmic-ray rejection was performed by interpolating over pixels with counts that were  $10\sigma$  above their neighboring pixels. We then improved the wavelength calibration by identifying the night-sky emission line peaks, and fitting a third order polynomial matching the measured wavelength of the peaks to their known wavelengths<sup>5</sup>. Sky subtraction was performed by means of a linear fit to the background counts in each CCD row along the cross-dispersion direction. In the fit, we used a  $3.5\sigma$ -clipping algorithm to remove outlier points due to residual cosmic rays and bad pixels.

In all cases, the galaxy light is blended with the light from the quasar images. Due to the different colors of the components and the faintness of the galaxy relative to the quasar, conventional tracing of the positions of the spectra along the cross-dispersion direction may not work. In order to overcome this problem, we have designed our tracing algorithm as follows.

We trace the spectra by fitting the fluxes and widths of Gaussians models for each component in the slit as a function of wavelength, where the relative spatial positions of the Gaussians were fixed using high-precision astrometry from HST images of the lenses (Falco et al. 2001 and the CAS-

TLES database<sup>6</sup>). We extracted a spectrum at the position of the galaxy (contaminated by the quasar light) and a spectrum of the quasar from a position along the slit that is diametrically opposed to, and as far as possible from, the galaxy position, but still having sufficient signal-to-noise (S/N) ratio. The spectra were corrected for atmospheric extinction using standard extinction curves<sup>7</sup>, and flux calibrated using the standard star LTT1788. A “cleaned” galaxy spectrum (i.e., de-contaminated of quasar light) was obtained by subtracting a scaled version of the quasar spectrum from the blended galaxy spectrum. The proper scaling of each of the quasar spectra was found by visual inspection of the subtracted spectra of the galaxy, and by requiring that the quasar emission lines vanish from the decontaminated galaxy spectrum. The galaxy fraction in the blended quasar+galaxy spectrum was in the range  $\sim 0.04$  to  $\sim 0.9$ , with a median of  $0.25$ . Figures 2-8 show the spectra of the lensing galaxies for which we succeed in measuring redshifts. In the other four cases, low S/N in the galaxy spectrum, excessive contamination from the quasars, or other peculiarities of the spectrum (see below), prevented us from measuring secure lens redshifts.

Our extraction process is not free of complications. Lensed quasars show differences among lensed images in both the continua and the emission lines (e.g., Richards et al. 2004; Keeton et al. 2005). For example, in Fig. 9-a we show the Mg II  $\lambda 2800$  emission line of the two images of HE0047–1756. After matching the continua of the two quasar images to the same level, there is a 13% difference in the flux of the Mg II lines. This difference is not due to the galaxy. The total emission from the galaxy, most of which lies in our galaxy aperture rather than the quasar apertures, is only 10% that of the quasars, and the spectrum of the galaxy has no feature near the Mg II  $\lambda 2800$  emission line that could produce an apparent difference between the line and continuum of the quasar. Figure 9-b shows a second example, the spectra of both quasar images of Q1355–2257 in the vicinity of the Mg II  $\lambda 2800$  emission line. The line equivalent widths differ by about 60%. Such differences in quasar spectra can be the result of microlensing that is preferentially magnifying or demagnifying the continuum or the emission lines of the images (e.g., Schechter & Wambsganss 2002; Keeton et al. 2005), millilensing (e.g., Abajas et al. 2002; Lewis & Ibata 2004; Keeton et al. 2005), or intrinsic quasar variability (e.g., Kaspi et al. 2000; 2005) combined with the time delay between the images (about 50 days and 40 days for HE0047–1756 and Q1355–2257, respectively; Witt, Mao, & Keeton 2000). The spectral differences between the two images could affect the galaxy spectrum that is obtained by subtracting the spectrum of quasar A from the lensed spectrum at the galaxy position, which is located between images A and B (see Fig. 1). An example of this effect is seen in the spectrum of LBQS1009–025 (Fig. 7), in which a residual of the quasar’s C III]  $\lambda 1909$  emission line is left in the “cleaned” galaxy spectrum. Note that, in this case, the lensing galaxy is located on top of image B (see Fig. 1) and hence there is no choice but to use image-A for the subtraction.

The redshifts of each galaxy were obtained by cross correlating the spectrum with template local galaxy spectra from Kinney et al. (1996). For each galaxy we tried template spectral types from elliptical to Sc, or “mixes” of varying weights between two adjacent types. To each template we first ap-

<sup>5</sup> Sky line wavelengths were taken from <http://alamoana.keck.hawaii.edu/inst/lris/skylines.html>

<sup>6</sup> <http://cfa-www.harvard.edu/castles/index.html>

<sup>7</sup> <http://www.eso.org/>

TABLE 1  
LOG OF OBSERVATIONS

Object Name	# of Exp.	Exp. time [sec]	Date	Seeing (Min..Median..Max) ["]	PA [deg]
HE0047–1756	1	1800	15-10-2004		
	1	1800	13-11-2004		
<i>total</i>	2	3600		0".64..0".73..0".82	0.47
PMNJ0134–0931	1	1200	13-11-2004	0".79..0".79..0".79	–52.52
HE0230–2130	1	1800	11-11-2004	0".87..0".87..0".87	–30.38
HE0435–1223	1	900	14-12-2004	0".75..0".75..0".75	–12.20
SDSS0924+021	2	2900	14-12-2004		
	2	2900	15-01-2005		
<i>total</i>	4	5800		0".62..0".71..1".39	10.83
BRI0952–0115	6	6350	05-01-2005		
	4	5800	14-01-2005		
<i>total</i>	10	12150		0".63..0".77..1".03	55.78
LBQS1009–025	2	2900	08-01-2005		
	4	5800	14-01-2005		
<i>total</i>	6	8700		0".68..0".78..1".05	24.95
Q1017–207	2	2900	12-01-2005		
	2	2900	15-01-2005		
<i>total</i>	4	5800		0".65..0".79..0".90	–86.65
Q1355–2257	3	4350	04-02-2005		
	2	2900	14-03-2005		
<i>total</i>	5	7250		0".71..1".01..1".26	81.03
PMNJ1632–003	2	2900	14-03-2005	0".57..0".63..0".68	–57.60
WFIJ2033–472	1	1800	15-10-2004	0".71..0".71..0".71	48.72

NOTE. — For objects that were observed on more than one night, the last line gives the total number and total time of exposures.

plied the redshift and then the Galactic extinction (Schlegel, Finkbeiner, & Davis 1998) toward the lens. In one case, PMNJ0134–0931, the lensing galaxy was not detected directly (by the procedure described above), but several absorption lines are visible in the quasar spectrum. In this case, we subtracted from the quasar spectrum a smoothed version of itself, and compared the resulting absorption line spectrum with a similarly normalized galaxy template.

Figures 2-8 show, along with the spectra of the lensing galaxies, also the best matching galaxy templates. The measured redshifts of the lensing galaxies, the Galactic extinctions (Schlegel et al. 1998), and the quasar redshifts, are summarized in Table 2. The redshifts of two of the lensing galaxies have been previously measured. The lens redshift of PMNJ0134–0931 was previously measured to be  $z = 0.7645$ , by Hall et al. (2002, based on the H&K Ca II absorption) and by Kanekar & Briggs (2003, based on 21 cm HI absorption). During the course of our VLT program, the lensing galaxy redshift in HE0435–1223 was measured by Morgan et al. (2005) to be  $z = 0.4546 \pm 0.0002$ . In both cases, we confirm the measured redshifts.

Although the continuum slopes and absorption features of three of the lens galaxies are best fit by spiral, rather than elliptical or S0 templates, in most cases there is evidence that the lens galaxies are nevertheless early types, which at high redshifts may have bluer colors than those of local ellipticals, probably due to some post-starburst signatures. Indeed, the [O III] emissions lines in the spiral templates are always absent in the lens galaxies, indicating a lack of ongoing star formation. In two cases, the intrinsically blue color may be compounded by some mild distortion of the continuum slope as a result of differential atmospheric refraction affecting our spectra, which were obtained at a non-parallactic angle. The observational and evolutionary effects are both discussed on a

TABLE 2  
LENSING GALAXIES - MEASURED REDSHIFTS

Object Name	$z_{lens}$	Galactic $E_{B-V}$	$z_{QSO}$
HE0047–1756	0.408	0.022	1.67
PMNJ0134–0931	0.766 <sup>a</sup>	0.031	2.216
HE0230–2130	0.522	0.022	2.162
HE0435–1223	0.455 <sup>b</sup>	0.068	1.689
SDSS0924+021	0.393	0.055	1.524
BRI0952–0115		0.063	4.426
LBQS1009–025	0.871	0.034	2.74
Q1017–207	1.088?	0.046	2.545
Q1355–2257	0.48?	0.072	1.373
PMNJ1632–003	1.165?	0.098	3.424
WFIJ2033–472	0.658	0.047	1.66

NOTE. — The uncertainty in redshift for all lenses is  $\sim 0.001$ , and is dominated by the error in the cross correlation, with a smaller contribution from the wavelength calibration uncertainty. The cross-correlation uncertainty was estimated based on a  $\Delta\chi^2$  test.

<sup>a</sup>Redshift previously measured by Hall et al. (2002), and Kanekar & Briggs (2003).

<sup>b</sup>Redshift previously measured by Morgan et al. (2005)

case by case basis in §3.

### 3. NOTES ON INDIVIDUAL OBJECTS

**HE0047–1756:** A doubly imaged lensed quasar discovered by Wisotzki et al. (2004), with an image separation of 1".44. The continuum and absorption features of the lens galaxy spectrum, shown in Fig. 2, are best matched by an Sb+Sc template (with a mix ratio of 9 : 1), at redshift  $z = 0.408$ . We note, however, that the emission lines in the template are absent from the lens galaxy spectrum. To investigate the source of this disparity, we have first examined whether

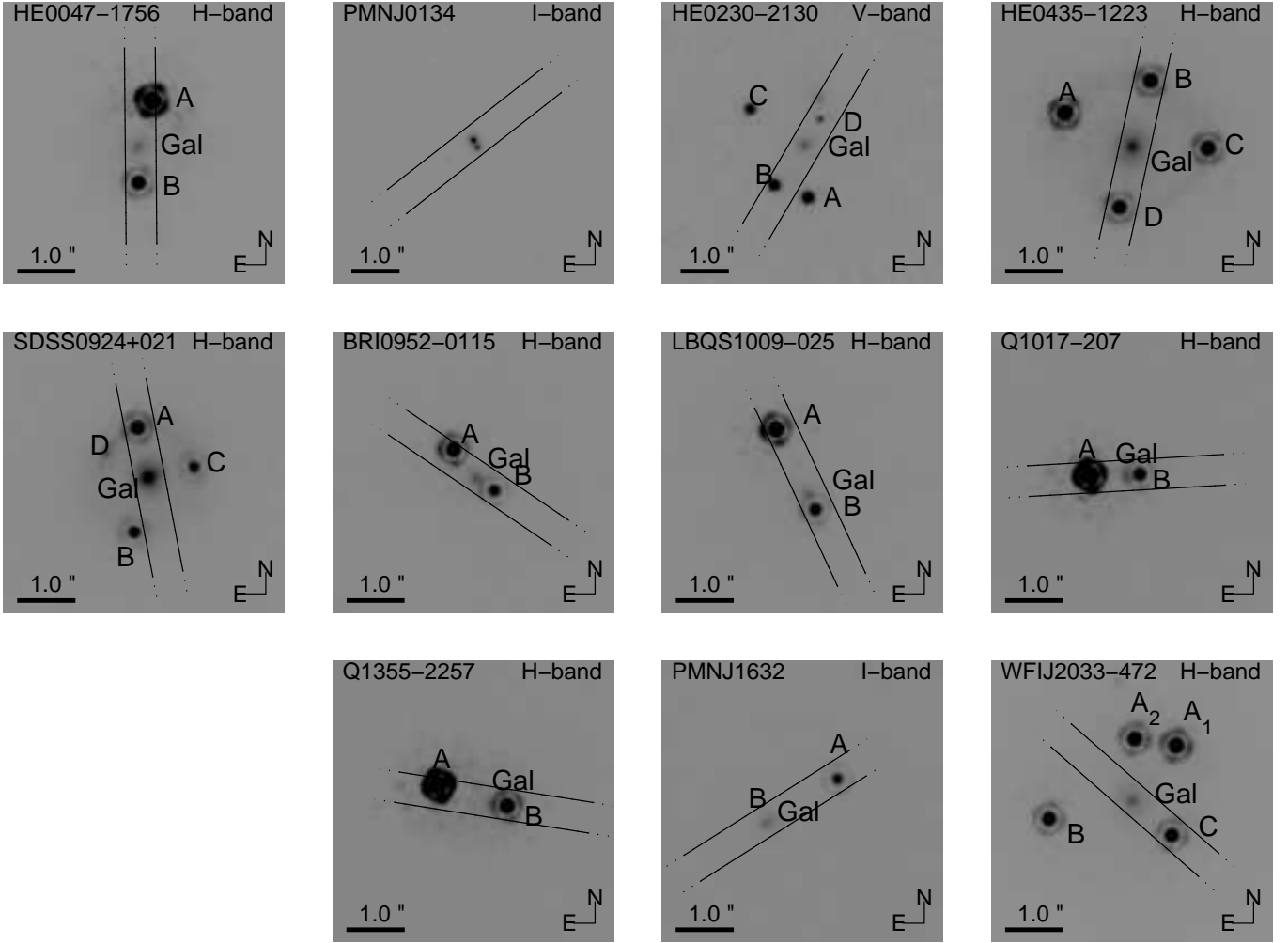


FIG. 1.— HST images of the lensed systems. The VLT/FORS2 slit orientations, and actual slit widths are overlaid.

the blue color of the lens galaxy could be the result of light loss through the slit, as a result of the differential atmospheric refraction<sup>8</sup> (Fillipenko 1982) and the non-parallactic slit angle that we used. We have estimated at  $\lesssim 15\%$  the possible change in spectral slope due to such light loss, for the particular slit angle, declination, observed hour angles and seeing widths appropriate for each exposure of this object. The corresponding difference in spectral slopes between the best-fit template and that of an elliptical galaxy is  $\sim 70\%$ . Furthermore, since the slit-centering acquisition images were obtained in the  $z$  band, we would expect that atmospheric refraction would lead to blue, rather than red, light loss, and hence to a reddening of the continuum. The blue color is therefore unlikely to be an observational defect.

A rough test of whether the mass of the lens is consistent with that of a normal spiral galaxy can be obtained by evaluating the velocity dispersion of a singular isothermal sphere (SIS) that would produce the observed image separation, given the source and lens redshifts,

$$\sigma_{\text{SIS}}^2 = \frac{c^2}{4\pi} \frac{D_s}{D_{ls}} \frac{\theta}{2}, \quad (2)$$

where  $\theta$  is the image separation. For the case at hand,  $\sigma_{\text{SIS}} \approx$

$190 \text{ km s}^{-1}$ , which is typical of early-types, but somewhat large for spirals. Along with the absence of indications of ongoing star formation, this argues that the lens galaxy is of early type. Its relatively blue color may then be the result of post-starburst signatures that are still present at the  $\sim 4$  Gyr lookback time.

**PMNJ0134–0931:** A highly reddened lensed quasar with a complex radio morphology, discovered by Winn et al. (2002a). The quasar is at redshift  $z = 2.216$ . The two brightest images are separated by  $0''.15$  (see Fig. 1). The lensing galaxy redshift was measured by Hall et al. (2002) and by Kanekar & Briggs (2003) and found to be  $z = 0.7645$ . This is consistent with our result,  $z = 0.766 \pm 0.001$ , based on the spectrum shown in Fig. 3.

**HE0230–2130:** Discovered by Wisotzki et al. (1999), this is a quadruply lensed quasar with redshift  $z = 2.162$  and a maximum image separation of  $2''.1$ . The lensing galaxy spectrum, shown in Fig. 4, is well matched by an equal mix of a S0 and Sa templates, with a redshift of  $z = 0.522$ . Following the same test as in the case of HE0047–1756, above, we find that the non-parallactic slit angle could lead to a change in slope of  $\lesssim 30\%$ , and as before, this would likely be in the sense of making the object redder. Between the S0 and Sa templates, the slope in the observed frame  $6000\text{--}8500 \text{ \AA}$  range changes

<sup>8</sup> <http://www.eso.org/gen-fac/pubs/astclim/lasilla/diffrefr.html>

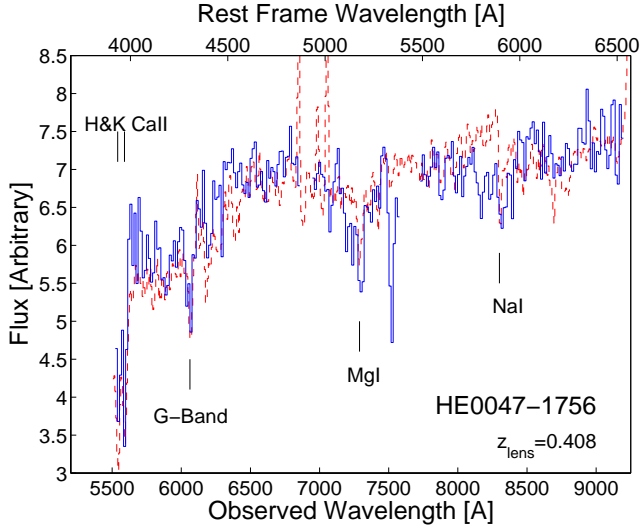


FIG. 2.— VLT/FORS2 spectrum, in the observer frame, of the lensing galaxy (solid line) of HE0047–1756, after subtraction of the contaminating quasar light. The dashed line shows the best fit galaxy template, after redshifting and correcting for Galactic extinction (Schlegel et al. 1998). The main absorption features are marked. Sections of the spectrum with strong telluric absorptions (6860–6930 Å and 7580–7720 Å) have been excised from the spectrum.

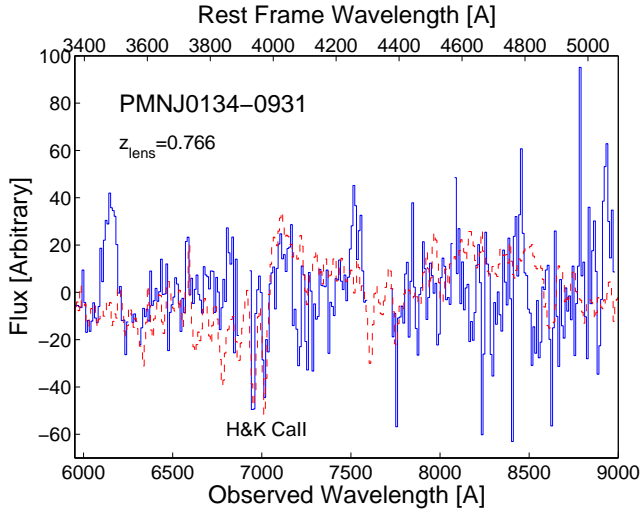


FIG. 3.— Spectrum of the lensing galaxy in PMNJ0134–0931 (solid line), after subtraction of a highly smoothed version of itself. The dashed line shows a galaxy spectral template after subtraction of a smoothed version of itself, normalized to have a similar variance as the spectrum of the lensing galaxy.

by  $\sim 70\%$ . Thus, observational effects could possibly play a partial role in the blue color of the lens galaxy. In terms of galaxy mass, the derived SIS velocity dispersion in this case is  $\sigma_{\text{SIS}} \approx 240 \text{ km s}^{-1}$ , which would be highly unusual for a spiral galaxy. We conclude that the lens galaxy is of early type with a blue color probably due to its being observed at a lookback time of 5 Gyr.

**HE0435–1223:** Discovered by Wisotzki et al. (2002), with a quasar redshift of 1.689. This is a quadruply lensed system with a maximum image separation of  $2''.6$ . The lens redshift was recently measured at  $z = 0.4546$  (Morgan et al. 2005). We confirm this result and find that the galaxy spectrum, presented at Fig. 5, is well matched by an S0 template.

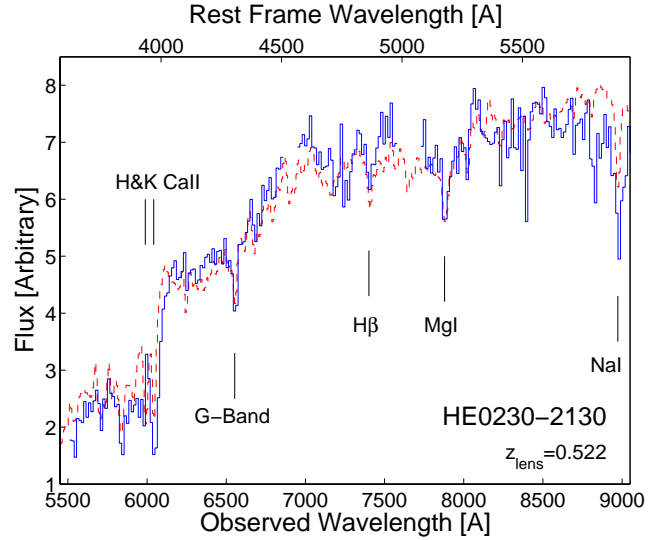


FIG. 4.— Same as Fig. 2, for HE0230–2130.

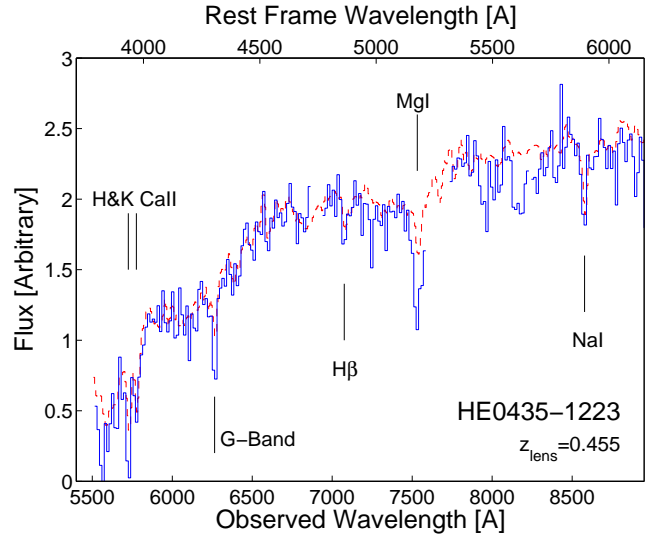


FIG. 5.— Same as Fig. 2, for HE0435–1223.

**SDSS0924+021:** Discovered as part of the Sloan Digital Sky Survey by Inada et al. (2003). This is a quadruply lensed quasar with a maximum image separation of  $1''.8$ , in which the merging pair (images A & D in Fig. 1) has a broad-band flux ratio of 10 – the most extreme known case of a “flux ratio anomaly” (see Keeton et al. 2005, for implications). The lensing galaxy spectrum, shown in Fig. 6, is well matched by an E galaxy template, with a redshift of 0.393.

**BRI0952–0115:** A doubly imaged quasar, with  $1''.0$  separation, discovered by McMahon & Irwin (1992). At  $z = 4.426$  (the redshift measurement was refined by Storrie-Lombardi et al. 1996), this is the highest redshift lensed quasar known. The “fundamental-plane redshift” of the lensing galaxy is  $z = 0.41 \pm 0.05$  (Kochanek et al. 2000). Storrie-Lombardi et al. (1996) identified several metal absorption systems, at redshifts of 1.993, 3.294, 3.475, 3.719, and 4.024 in the spectrum of the lensed quasar, one or more of which could contribute to the lensing. We note, however, that if these absorbers indeed

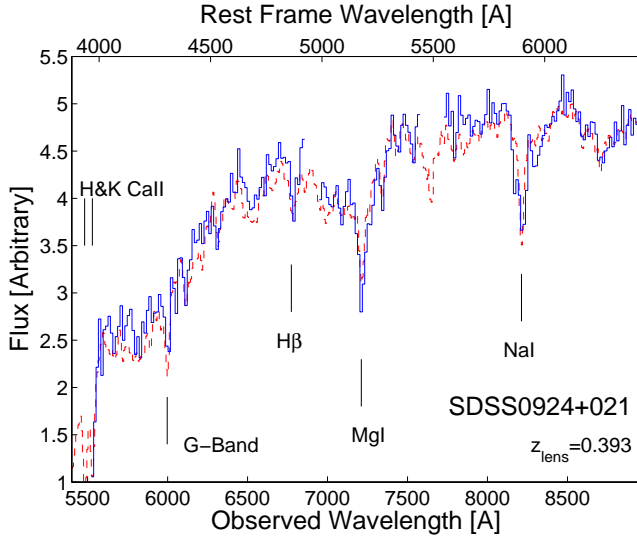


FIG. 6.— Same as Fig. 2, for SDSS0924+021.

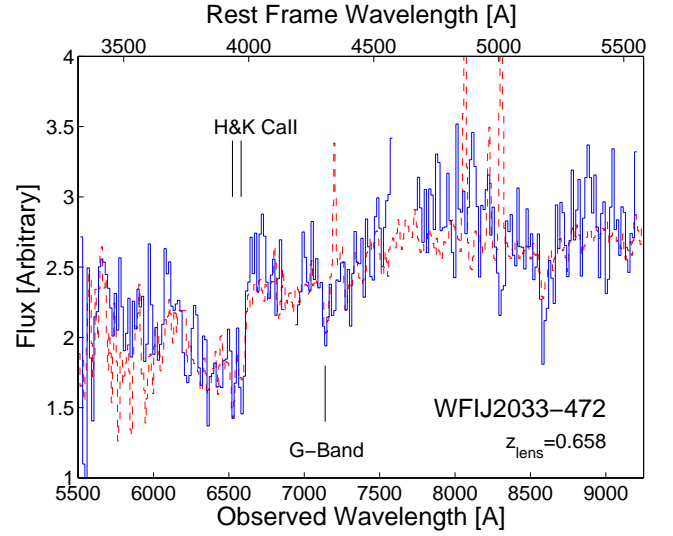


FIG. 8.— Same as Fig. 2, for WFIJ2033-472.

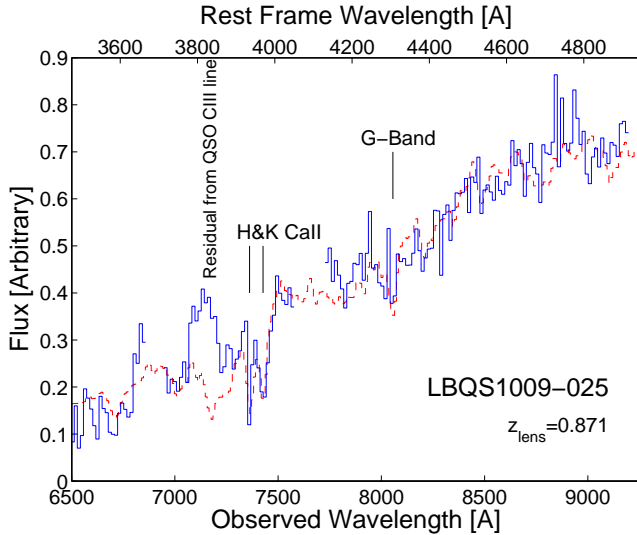


FIG. 7.— Same as Fig. 2, for LBQS1009-025.

contribute to the lensing then the fundamental-plane redshift may be biased toward lower redshifts. Even with over 3 hours of exposure time, the signal from the galaxy is too low to securely identify any features in the spectrum.

**LBQS1009-025:** A doubly imaged quasar, with  $1''.54$  image separation, discovered by Hewett et al. (1994). The quasar is at a redshift of 2.74. The lensing galaxy spectrum, shown in Fig. 7, is matched by an E galaxy template with a redshift of 0.871, very close to the fundamental-plane redshift (0.88) found by Kochanek et al. (2000).

**Q1017-207:** A doubly imaged quasar, with  $0''.85$  image separation, discovered by Claeskens et al. (1996). The quasar is at a redshift of 2.545 and the fundamental-plane redshift of the lensing galaxy is  $z = 0.78 \pm 0.07$  (Kochanek et al. 2000). Due to limited S/N (only 1.6 hr, of a requested 4.0 hr exposure time, were actually obtained) we fail to identify the type or redshift of the lens galaxy. Claeskens et al. (1996) detected a Mg II  $\lambda 2800$  absorber, with  $z = 1.085$ , in the com-

bined spectra of the images, and suggested that it could be due to the lensing galaxy. Surdej et al. (1997) obtained HST Faint Object Spectrograph (FOS) spectra of both images and detected the Mg II absorber only in the spectrum of image A. In our VLT spectra, the Mg II absorber is apparent in both images, and we refine its redshift to  $z = 1.088 \pm 0.001$  (Fig. 11). The absorption equivalent widths are  $9.4 \text{ \AA}$  and  $5.5 \text{ \AA}$  (observed frame) for image A and B, respectively. After correcting for the expected contamination by image A, we estimate that the Mg II absorption equivalent width in image B is  $4.2 \text{ \AA}$  (observed frame). The correction was made by calculating the ratio between the blended flux of image B (in the  $5700 - 5800 \text{ \AA}$  range), to the expected flux of image A at the same cross-dispersion position, based on the point-spread-function wing of image A on the side opposite to image B. By inspecting the HST-FOS spectra (Fig. 2 in Surdej et al. 1997), we estimate that the S/N ratio of the VLT spectrum is 10–20 times higher than that of the HST/FOS spectra. This may explain the absence of the Mg II absorber in image B in the HST/FOS spectra. If, as we suspect, the Mg II absorber is indeed present in the image B spectrum, the physical separation at the redshift of the absorber, about 7 kpc, suggests that the absorber is a massive galaxy capable of being the lens.

**Q1355-2257:** A doubly imaged quasar, with  $1''.23$  image separation, discovered by Morgan et al. (2003). The quasar is at a redshift of 1.373. Based on the flux of the galaxy and the Faber-Jackson (1976) relation, Morgan et al. (2003) estimated that the lens galaxy lies in the redshift range  $0.4 < z < 0.6$ , and suggested that the Mg II  $\lambda\lambda 2796, 2803 \text{ \AA}$  absorption feature at  $z = 0.48$  identified in their HST/FOS spectra of the system, could be associated with the lens galaxy. We note that our spectrum of quasar B, which would capture the most flux from the lens galaxy, shows an excess of emission relative to quasar A at wavelengths longward of  $\sim 5870 \text{ \AA}$  (see Fig. 9). This roughly corresponds to the wavelength at which a  $z = 0.48$  galaxy would have its  $4000 \text{ \AA}$  break.

**PMNJ1632-003:** A doubly imaged quasar, with  $1''.47$  image separation, discovered in radio frequencies by Winn et al. (2002b). The quasar is at a redshift of 3.424, and is the only quasar lensed by a galaxy for which the demagnified central

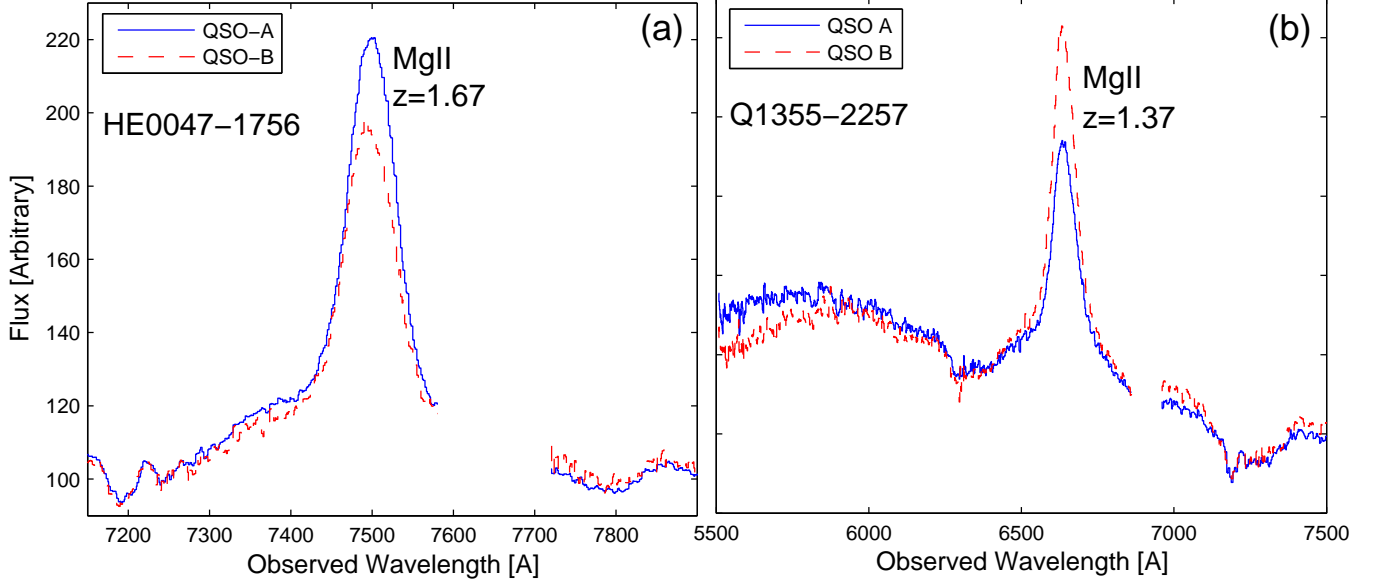


FIG. 9.— The Mg II  $\lambda 2800$  emission lines of the two lensed quasar images in HE0047–1756 (panel a) and in Q1355–2257 (panel b). After the continua are scaled to match each other, there are 13% and 60% differences, respectively, in the emission line fluxes of the two systems. The spectral differences could be due to microlensing, millilensing, or intrinsic quasar variability coupled with the time delay between images. The spectra of Q1355–2257 diverge from each other shortward of  $\sim 5870$  Å, which is the expected wavelength of the Balmer discontinuity of a  $z = 0.48$  galaxy (see text).

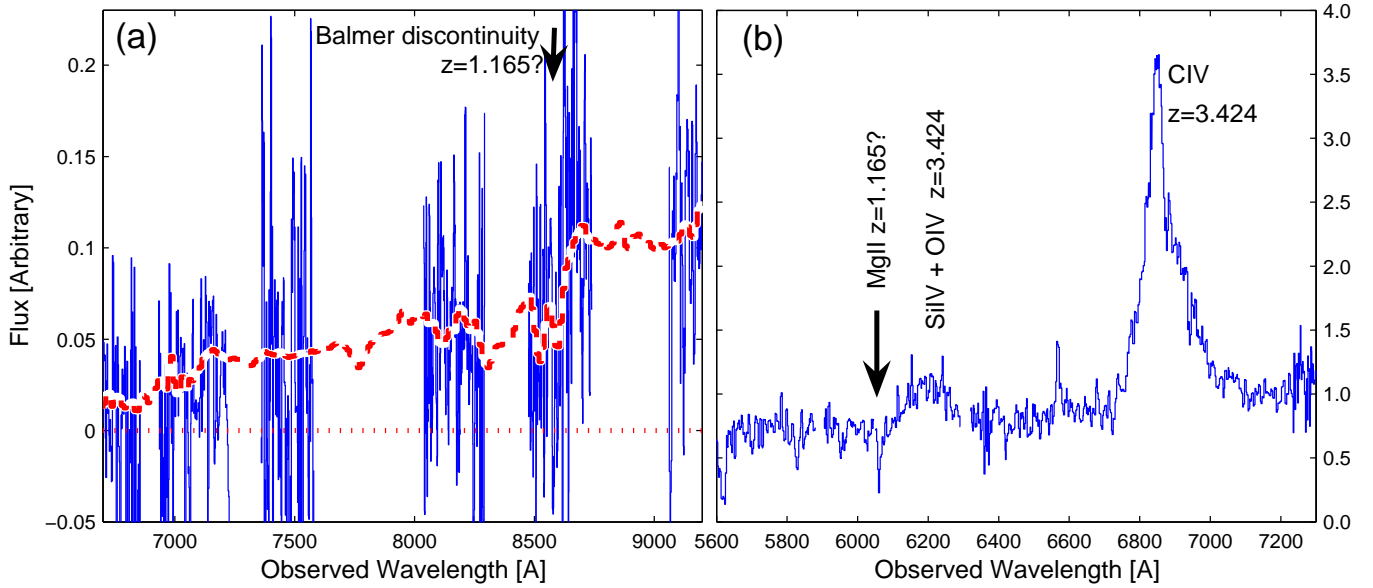


FIG. 10.— Panel a: Lens galaxy spectrum for PMNJ1632–003. Gaps in the spectra correspond to regions with very low S/N, due to atmospheric emissions, which we do not display for the sake of clarity. The dashed line is an elliptical galaxy template, redshifted to  $z = 1.165$ . Panel b: Spectrum of image-A of the lensed quasar PMNJ1632–003. The absorption at  $6060$  Å could be Mg II  $\lambda 2800$  Å, at the redshift suggested by the break seen in the galaxy spectrum in panel (a).

image has been securely detected (Winn et al. 2004). The existence of the central image sets a lower limit on the galaxy’s surface density at the location of the central image. The spectrum of the lensing galaxy is noisy and we cannot confidently identify the redshift. However, as seen in Fig. 10-a, we detect a jump in the spectrum at  $\sim 8600 \pm 40$  Å. If attributed to the Balmer discontinuity, then an absorption line at  $6060$  Å in the QSO spectrum (Fig. 10-b) may be Mg II  $\lambda 2800$  Å, and the galaxy redshift would be 1.165.

**WFLJ2033–472:** A quadruply lensed quasar, discovered by Morgan et al. (2004). The quasar redshift is 1.66 and the

maximum image separation is  $2''.5$ . The lensing galaxy spectrum, shown in Fig. 8, is matched by an Sb and Sc galaxy template (mix ratio of 4 : 1) with a redshift of 0.658. As in the cases of HE0047–1756 and HE0230–2130, above, the non-parallactic slit angle could lead to a change in slope of  $\lesssim 30\%$ , and as before, this would likely be in the sense of making the object redder. Between the S0 and Sb/Sc templates, the slope in the  $6000\text{--}8500$  Å range changes by  $\sim 75\%$  and therefore differential atmospheric refraction is unlikely to be the main cause of the blue color of the lens galaxy. The derived SIS velocity dispersion in this case is  $\sigma_{\text{SIS}} = 300 \text{ km s}^{-1}$ , corre-



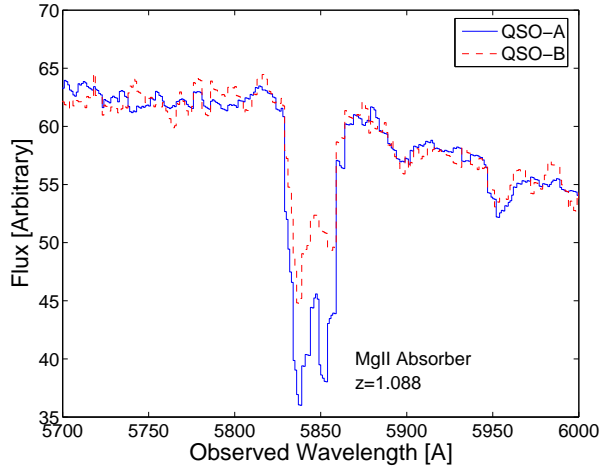


FIG. 11.— Section of the spectra of the two lensed images of Q1017–207, after the continua are scaled to match each other. A Mg II absorber at  $z = 1.088$  is detected in the spectra of both images, and given the expected blending, we suspect that the absorber is present in both images (see text).

sponding to a massive elliptical or a galaxy group. As in the previous two cases, the spiral-galaxy-like slope and absorption features in the lens galaxy spectrum most probably do not indicate a spiral galaxy lens.

To summarize, we have obtained low resolution VLT/FORS2 optical spectra of 11 gravitationally lensed quasar systems, and we have measured the redshifts of seven of the lensing galaxies. In three cases, the best spectral fits correspond to local spiral galaxy templates in terms of continuum shape and absorption feature depths. However, in all three cases we have argued that the lens galaxies are actually of early-type, based on the absence of emission lines, and on the large image separations that they produce, which are characteristic of massive ellipticals. In each case, we have also argued against a dominant observational source for the anomalous colors, and concluded that these early-type galaxies, as viewed at lookback times of  $\sim 5$  Gyr, are intrinsically blue. Their observed spectra likely carry the traces of previous episodes of star formation. Our fairly high success rate in obtaining spectroscopic redshifts, shows that full redshift information can be gathered for most lensed quasar systems. As discussed in §1, this information will be useful for a host of cosmological applications.

We thank Dovi Poznanski, Orly Gnat, and Shai Kaspi, for valuable discussions. This work was supported by a grant from the German Israeli Foundation for Scientific Research and Development.

#### REFERENCES

- Abajas, C., Mediavilla, E., Muñoz, J. A., Popović, L. Č., & Oscoz, A. 2002, *ApJ*, 576, 640
- Chae, K. 2003, *MNRAS*, 346, 746
- Chae, K., & Mao, S. 2003, *ApJL*, 599, L61
- Claeskens, J.-F., Surdej, J., & Remy, M. 1996, *A&A*, 305, L9
- Djorgovski, S., & Davis, M. 1987, *ApJ*, 313, 59
- Dressler, A., Lynden-Bell, D., Burstein, D., Davies, R. L., Faber, S. M., Terlevich, R., & Wegner, G. 1987, *ApJ*, 313, 42
- Faber, S. M., & Jackson, R. E. 1976, *ApJ*, 204, 668
- Falco, E. E., et al. 2001, *ASP Conf. Ser.* 237: Gravitational Lensing: Recent Progress and Future Go, 237, 25
- Filippenko, A. V. 1982, *PASP*, 94, 715
- Hall, P. B., Richards, G. T., York, D. G., Keeton, C. R., Bowen, D. V., Schneider, D. P., Schlegel, D. J., & Brinkmann, J. 2002, *ApJL*, 575, L51
- Hamana, T., Ohya, Y., Chiba, M., & Kashikawa, N. 2005, *ArXiv Astrophysics e-prints*, arXiv:astro-ph/0507056
- Hewett, P. C., Irwin, M. J., Foltz, C. B., Harding, M. E., Corrigan, R. T., Webster, R. L., & Dinshaw, N. 1994, *AJ*, 108, 1534
- Inada, N., et al. 2003, *AJ*, 126, 666
- Kanekar, N., & Briggs, F. H. 2003, *A&A*, 412, L29
- Kaspi, S., Smith, P. S., Netzer, H., Maoz, D., Jannuzi, B. T., & Givon, U. 2000, *ApJ*, 533, 631
- Kaspi, S., Maoz, D., Netzer, H., Peterson, B. M., Vestergaard, M., & Jannuzi, B. T. 2005, *ApJ*, 629, 61
- Keeton, C. R., Kochanek, C. S., & Falco, E. E. 1998, *ApJ*, 509, 561
- Keeton, C. R. 2001, *ApJ*, 561, 46
- Keeton, C. R., Burles, S., Schechter, P. L., & Wambsganss, J. 2005, *ArXiv Astrophysics e-prints*, arXiv:astro-ph/0507521
- Kinney, A. L., Calzetti, D., Bohlin, R. C., McQuade, K., Storchi-Bergmann, T., & Schmitt, H. R. 1996, *ApJ*, 467, 38
- Kochanek, C. S., et al. 2000, *ApJ*, 543, 131
- Kochanek, C. S. 2002, *ApJ*, 578, 25
- Kochanek, C. S. 2004, *ApJ*, 605, 58
- Kochanek, C. S., Morgan, N. D., Falco, E. E., McLeod, B. A., Winn, J. N., Dembicky, J., & Ketzbeck, B. 2005, *ArXiv Astrophysics e-prints*, arXiv:astro-ph/0508070
- Leitherer, C., et al. 1999, *ApJS*, 123, 3
- Lewis, G. F., & Ibata, R. A. 2004, *MNRAS*, 348, 24
- Maoz, D. 2005, in "Impact of Gravitational Lensing on Cosmology", IAU Symposium 225, Eds. Y. Mellier and G. Meylan, (Cambridge: Cambridge University Press), p413
- Maoz, D., & Rix, H. 1993, *ApJ*, 416, 425
- McMahon, R., & Irwin, M. 1992, *GEMINI Newsletter Royal Greenwich Observatory*, 36, 1
- Méndez, R. H., Riffeser, A., Kudritzki, R.-P., Matthias, M., Freeman, K. C., Arnaboldi, M., Capaccioli, M., & Gerhard, O. E. 2001, *ApJ*, 563, 135
- Morgan, N. D., Gregg, M. D., Wisotzki, L., Becker, R., Maza, J., Schechter, P. L., & White, R. L. 2003, *AJ*, 126, 696
- Morgan, N. D., Caldwell, J. A. R., Schechter, P. L., Dressler, A., Egami, E., & Rix, H. 2004, *AJ*, 127, 2617
- Morgan, N. D., Kochanek, C. S., Pevunova, O., & Schechter, P. L. 2005, *AJ*, 129, 2531
- Ofek, E. O., Rix, H., & Maoz, D. 2003, *MNRAS*, 343, 639
- Pahre, M. A., Djorgovski, S. G., & De Carvalho, R. R. 2001, *Ap&SS*, 276, 983
- Richards, G. T., et al. 2004, *ApJ*, 610, 679
- Rusin, D., et al. 2003, *ApJ*, 587, 143
- Rusin, D., & Kochanek, C. S. 2005, *ApJ*, 623, 666
- Schechter, P. L., & Wambsganss, J. 2002, *ApJ*, 580, 685
- Schlegel, D. J., Finkbeiner, D. P., & Davis, M. 1998, *ApJ*, 500, 525
- Storrie-Lombardi, L. J., McMahon, R. G., Irwin, M. J., & Hazard, C. 1996, *ApJ*, 468, 121
- Surdej, J., Claeskens, J.-F., Remy, M., Refsdal, S., Pirenne, B., Prieto, A., & Vanderriest, C. 1997, *A&A*, 327, L1
- Treu, T., Stiavelli, M., Casertano, S., Möller, P., & Bertin, G. 2002, *ApJL*, 564, L13
- Treu, T., & Koopmans, L. V. E. 2002, *MNRAS*, 337, L6
- Treu, T., & Koopmans, L. V. E. 2004, *ApJ*, 611, 739
- van Dokkum, P. G., Franx, M., Kelson, D. D., & Illingworth, G. D. 1998, *ApJL*, 504, L17
- van Dokkum, P. G., Franx, M., Kelson, D. D., & Illingworth, G. D. 2001, *ApJL*, 553, L39
- Winn, J. N., et al. 2002a, *AJ*, 123, 10
- Winn, J. N., Lovell, J. E. J., Chen, H., Fletcher, A. B., Hewitt, J. N., Patnaik, A. R., & Schechter, P. L. 2002b, *ApJ*, 564, 143
- Winn, J. N., Rusin, D., & Kochanek, C. S. 2004, *Nature*, 427, 613
- Wisotzki, L., Christlieb, N., Liu, M. C., Maza, J., Morgan, N. D., & Schechter, P. L. 1999, *A&A*, 348, L41
- Wisotzki, L., Christlieb, N., Bade, N., Beckmann, V., Köhler, T., Vanelle, C., & Reimers, D. 2000, *A&A*, 358, 77
- Wisotzki, L., Schechter, P. L., Bradt, H. V., Heinmüller, J., & Reimers, D. 2002, *A&A*, 395, 17
- Wisotzki, L., Schechter, P. L., Chen, H.-W., Richstone, D., Jahnke, K., Sánchez, S. F., & Reimers, D. 2004, *A&A*, 419, L31
- Witt, H. J., Mao, S., & Keeton, C. R. 2000, *ApJ*, 544, 98